Development and Testing of an Unconventional Morphing Wing Concept with Variable Chord and Camber

Keidel, Dominic; Sodja, Jurij; Werter, Noud; De Breuker, Roeland; Ermanni, P.

Publication date
2015

Document Version
Final published version

Published in
Proceedings of the 26th International Conference on Adaptive Structures and Technologies

Citation (APA)
Keidel, D., Sodja, J., Werter, N., De Breuker, R., & Ermanni, P. (2015). Development and Testing of an Unconventional Morphing Wing Concept with Variable Chord and Camber. In M. Monajjemi, & W. Liang (Eds.), *Proceedings of the 26th International Conference on Adaptive Structures and Technologies: Kobe, Japan* Article ICAST2015 #83 ICAST.

Important note
To cite this publication, please use the final published version (if applicable).
Please check the document version above.

ICAST2015: 26th International Conference on Adaptive Structures and Technologies
October 14-16th, 2015, Kobe, Japan

ICAST2015 #83

Development and Testing of an Unconventional Morphing Wing Concept with Variable Chord and Camber

D. Keidel[1,2], J. Sodja[2], N. Werter[2], R. De Breuker[2*] and P. Ermanni[1]

[1] Laboratory of Composite Materials and Adaptive Structures, ETH Zurich, Switzerland
[2] Faculty of Aerospace Engineering, Delft University of Technology, The Netherlands

Abstract

Driven by the need to improve the performance and energy-efficiency of aircraft, current research in the field of morphing wings is growing in significance. The most recently developed concepts typically adjust only one characteristic of the wing. Within this paper a new concept for morphing wings is developed and tested, enabling large changes of the chord length and camber simultaneously. By changing two characteristics of the wing instead of one, the range of flight missions can be extended more effectively. To achieve these large shape changes, highly adaptable leading and trailing sections are mounted onto a rigid wingbox. A thin polymer film is encompassing these three sections. By adjusting the length of this film, the outline of the wing can be changed significantly. A prototype has been designed and manufactured for wind tunnel tests. The leading and trailing sections are made of polyurethane foam, which can be compressed to 10 percent of its original volume. Different polyurethane foams are tested for optimal stiffness to withstand the aerodynamic loads acting on the wing, while being soft enough to accommodate the large deformations. The film encompassing the sections is retracted into the wingbox to achieve the desired shapes of the airfoil. On the one hand, this film needs to be very thin to fit into the wingbox, while on the other hand it needs to be stiff enough to withstand the pressure exerted by the foam. The manufactured prototype enables changes of the chord length by 30 percent and the camber by 10 percent of the chord length. These deformations were achieved without any significant kinking or buckling. Three different asymmetric airfoil shapes and two symmetric shapes with different chord lengths were tested in a series of wind tunnel tests. All five airfoil shapes deformed very little under wind loads. The lift and drag results were compared to generate values and matched very closely. The prototype fulfils all predefined requirements and performs very well over a wide range of airfoil shapes and wind speeds.

1. INTRODUCTION

Ever since the first human heavier-than-air flight by the Wright brothers, shape morphing wings were used to control the flight dynamics of aircraft in various ways. As these early aircraft were built from wood and canvas, morphing of the control surfaces could be easily achieved by the pilot. As the size and, hence wing loading of aircraft increased, materials and construction changed to much more rigid designs. Therefore hinged control surfaces were introduced to guarantee full flight control. This enabled

* R.DeBreuker@tudelft.nl

larger and heavier aircraft to be build. However, the performance of these aircraft was less than optimal for a range of different flight conditions.

In more recent years new technologies and materials enabled the design and actuation of adaptive load carrying structures such as wings, as outlined by Sofla et al. [1]. In the case of full size aircraft, due to strict regulations, only small incremental changes take place. However, for small-scale UAV research is done using various techniques and materials. Using UAV for testing allows cheaper and faster concept validation. Different concepts aim to change different characteristics of the wing, or even the entire aircraft. These concepts can be split roughly into two categories. Slow deformation for different flight missions, and fast deformations for active flight and loads control. The reviewed literature, summarized in Section 1.1, encloses mainly concepts from the first category, as the focus of this project is to design and manufacture a wing which enables slow, but very large deformations.

The objective of this project is to evaluate the possibilities of large deformation with simultaneous chord and camber morphing. Therefore a new morphing wing concept is designed and developed. The idea is to mount flexible polymer foam sections onto a stiff wingbox. A very thin skin encompasses the foam sections and the wingbox. By changing the length of the skin, the shape and size of the wing is changed. The detailed concept is explained in Chapter 2. A fully functional small-scale wing is manufactured and tested in a wind tunnel. The novelty of the concept is the combination of materials used and the larger than usual morphing capabilities. In order to achieve the aimed for deformations, materials such as foam and thin polymer film are used.

1.1 Background

The two main morphing concepts related to this project are morphing of the chord length and camber morphing. For both morphing techniques various approaches have been outline by Sofla et al. [1] and Barbarino et al. [2], but there has been very little research on the combination of both.

Changing the chord length impacts different characteristics of a wing. Most notable it affects the aspect ratio. If the wing span is kept constant and the chord length is increased, payload increases and take-off and landing speeds decrease. The LIG-7 built by Bakshaev in 1937, is a full size aircraft which can extend or retract six sections along each wing. By extending the sections, the landing speeds decrease by 25%, while the take-off distance decreases by 45%. More recent research is done on UAVs, such as the NextGen MFX-1, by Flanagan et al. [3]. The MFX-1 achieves a range of different wing shapes by changing the sweep angle, wing span and chord length. Changing the chord length, without influencing any other parameters increases the weight of the wing drastically, while only marginally altering the flight characteristics.

Changing the camber of the wing has a much higher impact on the wings performance, than changing the chord length. While keeping all other parameters constant, changing the camber affects the generated lift and drag of the wing. Morphing of the camber is used for active flight control, as well as adapting to different flight missions. The Active Aeroelastic Wing (AAW) program by NASA uses camber morphing on a full-scale wing, as described by Pendleton et al. [4] The wing of the AAW program has a leading edge with optimized stiffness distribution in order to achieve shape changes. Small UAV wings, which can perform camber changes are described by Barrett et al. [5] and Good [6]. The shape changes are limited by the inner components and the stiffness of the skin. Another disadvantage of these projects is, that only the rearmost part of the wing is actively deformed, while keeping the remaining wing unchanged.

The most important materials to achieve both chord and camber morphing are the polymer foam and the thin skin material. The polymer foam needs to match a variety of criteria, in order to result

in a successful test wing. The foam needs to be stiff enough to withstand the wind and bending loads acting on the wing, while simultaneously being flexible enough to yield under the pressure of the skin. Furthermore, the stiffness of the foam needs to higher at the trailing edge to prevent the trailing edge of folding. According to Liu and Subhash [7], the compression behaviour of polymer foams can be generally split into three regions: (i) a linear elastic region; (ii) a plasticity-like stress plateau; and (iii) a densification region. The aim is to pre-compress the foam to the plasticity-like stress plateau, where it exerts roughly equal force on the skin during the entire compression. According to the stiffness of the foam, the skin material needs to be chosen. Thill et al. [8] summarizes different morphing skins and materials which themselves morphing. However, for this project the material needs to be very stiff with little elongation, as the material is rolled up, thereby morphing the shape of the wing. The skin needs to be strong enough to compress the foam, while being thin and flexible enough to be rolled up. In Section 2.3 different polymer foam and skin materials are evaluated and selected.

2. WING DESIGN AND MANUFACTURING

In order to go from an initial idea to a fully functional prototype, the wing concept is divided into sub-problems, which can be tackled separately. The prototype is manufactured using available facilities and materials and tested in a small sub-sonic low turbulence wind tunnel. The used materials are chosen based on certain criteria, such as durability, light-weight, cost, availability, and performance. Especially the foam and skin materials are tested in order to find an optimal combination of both, as there is little research on the combination of both in context with aircraft or wing design. In the following sections the design, shape and material evaluation are described in detail.

2.1 Concept Overview

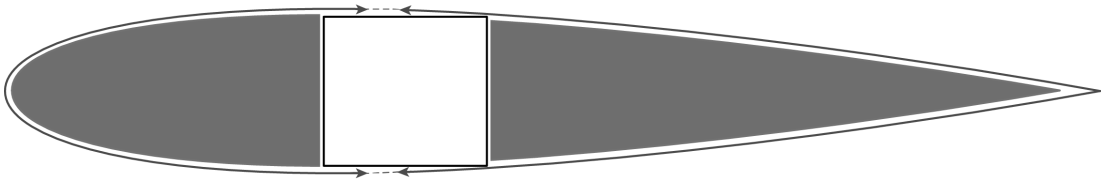

Figure 1. First basic concept idea (Grey: Foam encompassed by thin skin)

The underlying idea of this project is to develop a new morphing wing enabling large changes of the chord and camber. The idea is to split the airfoil into three main sections, as shown in Figure 1. The leading and trailing sections are made from very compliant foam and are mounted onto a rigid wingbox in the centre. All three sections are encompassed by a thin skin. The wingbox has an open cross section, which allows the skin to be retracted into the wingbox. By retracting the skin into the wingbox, the foam is compressed and the outline of the airfoil changes. As the skin can be retracted at each end individually, the airfoil can be morphed into different symmetric and asymmetric shapes with variable chord and camber. The shapes which are aimed for are described in Section 2.2. The skin is reeled onto a thin axle located in the wingbox, which in turn are actuated by stepper motors and controlled using an arduino micro controller. During the idea generation certain features are developed, which play a crucial role in the design of a functioning prototype. These features are outlined for clarity in the following list:

Foam Compartment The foam compartments are positioned between the wingbox and the leading and trailing foam sections. Each consists of a thin plate which pushes out the foam sections while the foam is extended. When the skin is retracted to fully compress the foam, the thin plates are retracted as well, thereby decreasing the overall cross section and the chord length of the airfoil in its compressed state.

Compartment Ledges In order to ensure a smooth outline if the airfoil, the hard edges of the compartment plates need to be smoothed out. In order to do so flexible ledges are introduced, which bend with the skin, but keep a smooth outline across the foam compartment. They span from the wingbox over the compartment plates.

Wing Mount The wing mount connects the wing to the balance during testing. Furthermore it keeps the motors in place. At the base of the wing mount two plates are mounted above each other and can be rotated to adjust the angle of attack of the wing.

End-Plates The end-plates are mounted at the root and the tip of the wing. They connect the wing to the wing mount. They further hold the guides of the compartment plates and some of the actuation in position. There are two sets of end-plates; one is the size of the wing, which simulates a finite wing, and the other extends outward from the wing, to simulate an infinite wing.

In order to find the best solution for this morphing wing, it is divided into sub-problems. These include: skin material, skin mounting, foam material, wingbox shape and design, and actuation. For each of these problems a variety of solutions is come up with. They are collected in a morphological box. From this, four different concepts are developed, incorporating different solutions. For these concepts, the functionality and interaction of the different components is assessed. The concepts are shown in Figure 2. The main difference between the concepts is the wingbox layout. Concept 1 has a stiff wingbox, with a fixed length, while the other concepts have flexible foam compartments, which decreases the overall length of the collapsed wing. The four concepts are evaluated using a list of criteria, with include: deformation from structural and aerodynamic loads, airfoil shape and deformation capabilities, and collapsibility. Based on this evaluation, concept 1 performs worst, while concepts 2 to 4 perform similarly well, due to the wingbox design and the materials used. For the final concept, the best aspects of each concept are combined. The wingbox is designed as small as possible, enlarging the foam compartments. The leading section foam is made of one part, while the trailing section includes a stiffer part made of styrofoam at the trailing edge, to ensure a sharp edge which maintains the aerodynamic performance. The skin is made of a very thin polymer film which takes up as little as possible volume within the wingbox, while being strong enough to prevent elongation. It is split into two parts, one for the leading section and one for the trailing section. The skin is reeled up onto four axles inside the wingbox, which are actuated separately by stepper motors. The compartment plates are actuated by strings, which are reeled up using servo motors for discrete positioning.

2.2 Airfoil Shape and Size

In order to define the exact size of the components, the airfoil shape and size needs to be defined. The undeformed and deformed airfoil shapes are chosen from the 4-digit NACA series. For this series of airfoil profile theoretical models for validation are available, which are used for comparison with the wind tunnel test results.

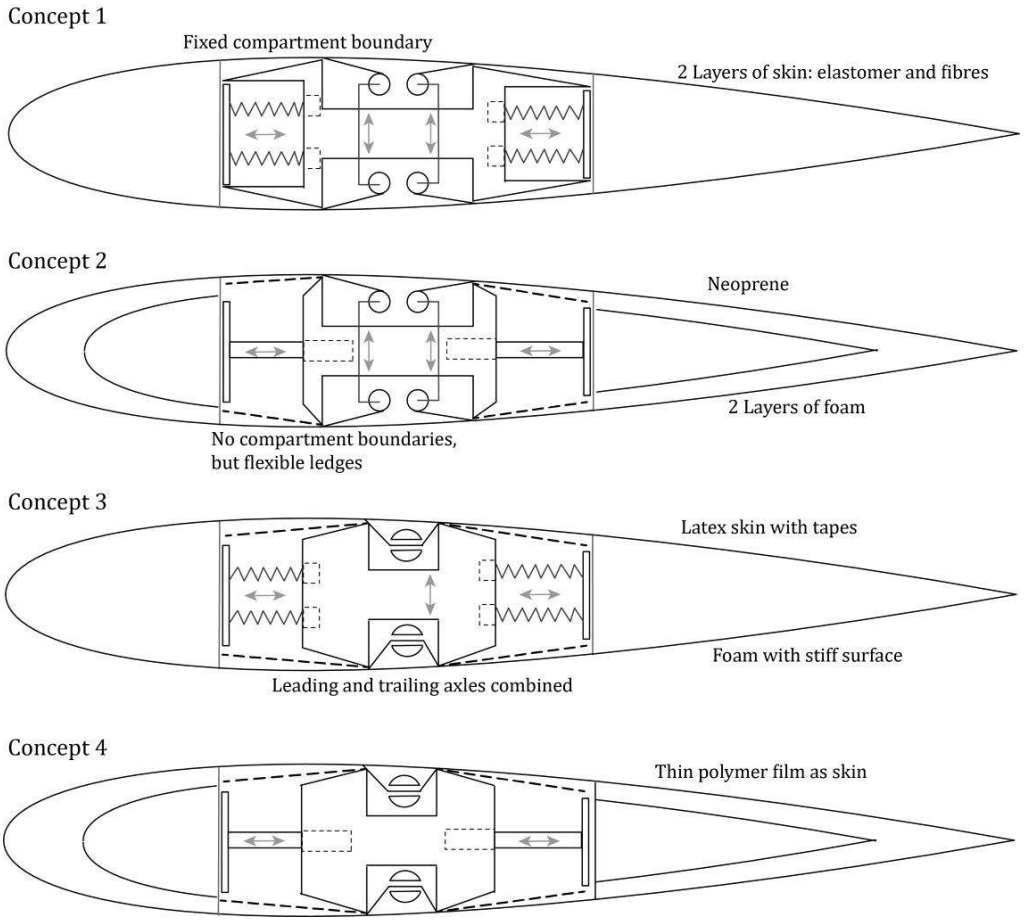

Figure 2. Four different concept ideas sketched out; dashed: flexible compartment ledges

As the used wind tunnel has a cross section of $400 \times 400mm$, the wing span is defined as $400mm$. The undeformed chord length is defined to be $300mm$ to maintain a large enough wingbox to contain the actuation mechanism.

The initial shape of the airfoil is chosen to be the NACA 0015 profile. This shape is chosen as a trade-off between induced drag and wingbox thickness. Compared to similar profiles, it has a very low induced drag over a range of lift coefficients, as shown in Figure 4. The maximum deformed shapes, which are tested are the NACA 0018 for symmetric shapes, and NACA 9315 for the asymmetric shapes. The asymmetric shape and the location of the wingbox are chosen, to minimize the concave curves at the underside of the wing, which the skin needs to achieve, as shown in Figure 3.

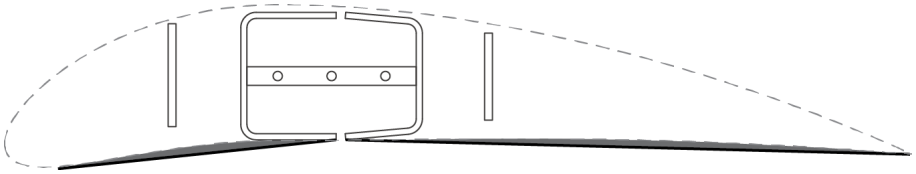

Figure 3. Concave curves of the skin on the underside of the wing are minimized

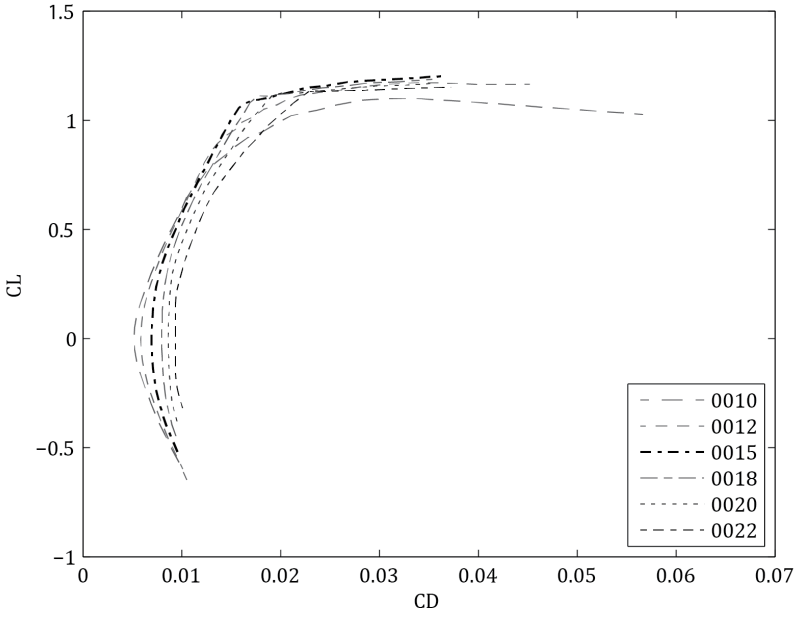

Figure 4. Theoretical lift-to-drag curves for different symmetric profiles

2.3 Material Evaluation

As a core component for successfully manufacturing and operating the wing, the foam material for the leading and trailing section is critical. Therefore, prior to testing the wing, different foams with different compression characteristics are evaluated. According to Liu and Subhash [7] polymer foam compression is split into three distinct regions: a linear elastic region; a plasticity-like stress plateau; and a densification region. After an initial linear elastic compression, the cell walls of the foam start to collapse, and the stress plateau is reached, where the stress stays roughly constant. After all cell walls have collapsed, the foam material starts to densify. For this project, the used foam shall only operate within the second region, the stress plateau, where the force exerted on the skin stays equal. If the foam is compressed to far, therefore reaching the densification regime, it will have a permanent effect on the consistency of the stress plateau. Different polymer foams with different characteristics are tested and compared, in order to find the best suited foam to use for the final wing. The test samples are $50 * 50 * 40mm$ and compressed multiple times to gain data on repetitive compression behaviour. From the different tested foams three materials are selected for further testing, which all have different stress plateau levels. The stress-strain curves for the first two compressions of the three chosen materials are shown in Figure 5. The required stress needed to compress the stiffest foam to the beginning of the densification phase is approximately $13 \times 10^{-3} N/mm^2$.

The skin of the wing has two crucial requirements to fulfil: (1) withstand the force acting from the foam, and (2) have a smooth and surface to minimize drag, while being flexible enough to be rolled up within the wingbox. The tested materials include different ethylene films (PFA, ET), and Kapton film. Each of the materials was tested for their tensile strength. The test results are shown in Figure 6. These tests show, that the Kapton film is most suited for the wing. The maximum yield stress, which the film can take is 45 N/mm^2.

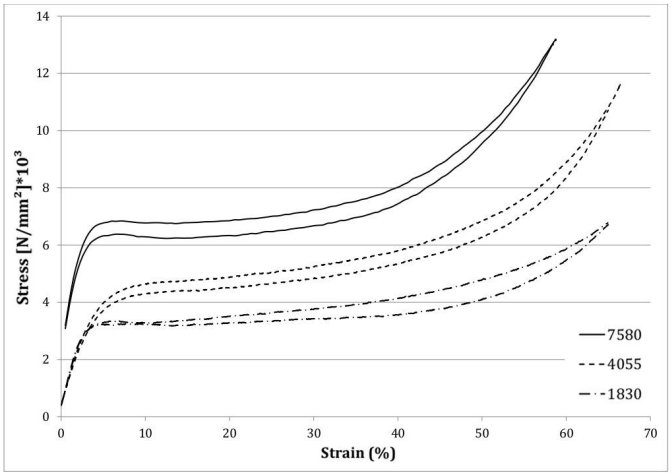

Figure 5. Stress-strain behaviour of the selected foams

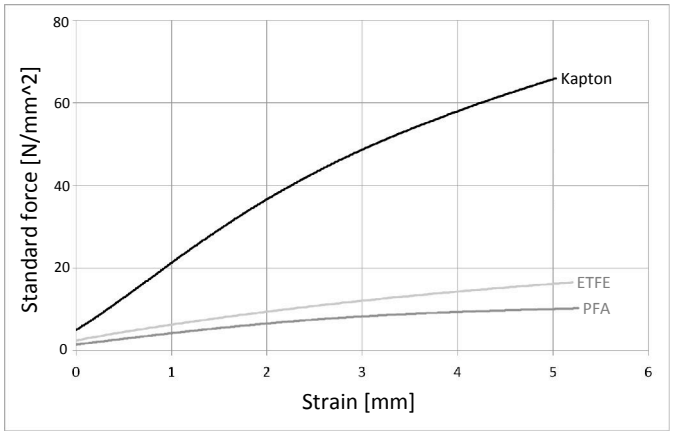

Figure 6. Stress-strain curves of the tested skin materials

The force required to compress the foam is equal to $F_{comp} = \sigma \times Area$ which is equal to $F_{comp} = 13 \times 10^{-3} \times 400 \times 30 = 156N$. The force that can be exerted by the skin without any permanent elongation is $F_k = \sigma \times Area$ which results in $F_k = 457.2N$. However, the skin is not pulled parallel to the film, but at an angle. Therefore the force, which can be exerted on the skin needs to be corrected. It is assumed, that when the foam is fully compressed, the angle between the skin and the x-axis is 45°. The corrected force is calculated using a safety factor of two:

$$F_{k,corr} = \frac{F_k \times cos(45)}{f_S}$$
$$F_{k,corr} = \frac{457.2 \times cos(45)}{2} = 161.6N$$

Therefore, the force which can be exerted on the kapton film is greater than the force required to compress the foam, as $161.6N > 156N$.

3. WIND TUNNEL EXPERIMENTS

According to the decisions taken in Chapter 2, the wing is manufactured and assembled. The finished, fully functional prototype is shown in Figure 7. The trailing foam section is slightly modified, as the trailing edge keeps collapsing. The polymer foam is to thin to exert enough force on the skin to keep the desired shape. Therefore the foam section is split into two parts. The front part remains polymer foam, while the rear part is replaced with a small styrofoam wedge. If the trailing edge has a rounded or blunt shape, it has a very negative effect on the lift and drag characteristics., as it creates turbulences. The wing is tested in a wind tunnel in order to compare the prototypes performance to the predicted lift and drag characteristics, generated using xfoil, an aerodynamic analysis code. The test setup and testing is described in the following sections.

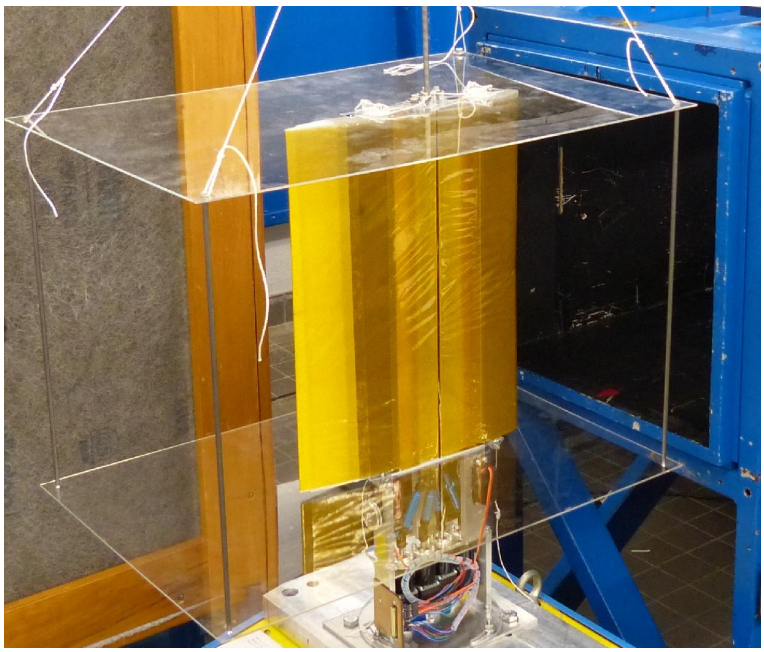

Figure 7. Fully-functional test wing mounted in the wind tunnel with the infinite end-plates

3.1 Test Setup

A subsonic, low turbulence open wind tunnel with a cross section of $400 \times 400mm$ is used for the wind tunnel tests. The wind speed is measured using a venturi nozzle which is placed in the wind tunnel ahead of the test wing. As it is an open wind tunnel some correction factors need to be incorporated to compare the tests with the xfoil predictions, which are explained in Section 3.2.

The wing is tested in five different wingshape configurations: NACA0015, NACA0018, NACA3315, NACA6315, NACA9315. The angle of attack is varied between $0°$ and $18°$, in intervals of $3°$. The wing is tested at wind speeds between 8 and 18 m/s. Therefore the Mach number varies from 0.0233 to 0.0525, and the Reynolds number varies from 180,000 to 360,000. Each shape is tested over the range of angles of attack and wind speeds to attain more significant data. Each of the experiments over a range of wind speeds and angles of attack is repeated, in order to obtain more representative data.

In order to fully understand the behaviour of the test wing, different end-plates are tested in the wind tunnel. The first set of end-plates is roughly the outline of the wing, to simulate a finite wing, therefore named finite end-plates. The second set of end-plates extends the complete width of the wind tunnel and twice along the chord length. These simulate an infinite wing which theoretically generates more lift, as less lift is lost at the wing tips and are called infinite end-plates. The end-plates are connected to the wing and the balance and therefore increase the measured drag of the wing. The used balance measures forces and moments in x,y,directions. The moments are used to validate the measured forces. Because the entire wing, including the end-plates and wing mount are connected to the balance, the forces acting on everything are measured. Therefore the drag of the end-plates needs to be taken into account as well.

3.2 Theoretical Predictions

In order to attain validated data, which the wind tunnel test results can be compared to, the analysing tool xfoil is used. As the NACA profiles are predefined in the xfoil program the generated data is assumed to be valid and accurate. The theoretically predicted lift and drag curves only differ slighty when varying the Mach and Reynolds number. Therefore, the average wind speed of 13 m/s is used to generate the lift and drag curves, which the wind tunnel tests are compared to. For angles of 12° and above certain lift characteristics change but these are disregarded as these values tend to be very inaccurate due to the fact that the used wind tunnel has an open test section.

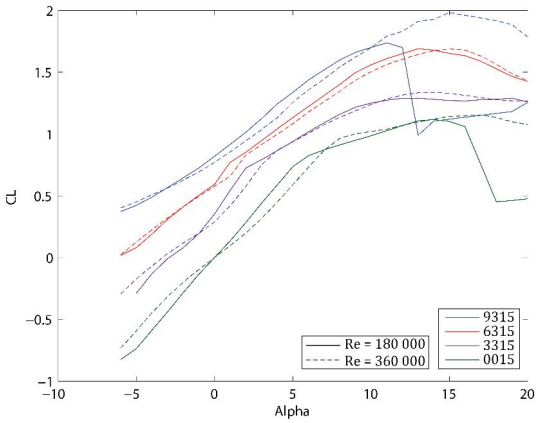

Figure 8. Change in lift coefficient depending on the Reynolds number

The open test section of the wind tunnel needs to be accounted for in the theoretical model, as the shape and size of the wing significantly influence the air flow of the wind tunnel. There are two factors that need to be accounted for to compare the wind tunnel tests to the theoretical predictions. Firstly, the difference between the geometric angle of attack α and effective angle of attack α_{eff} affects lift and drag measurements. The local flow direction near the wing changes depending on various factors, such as aspect ratio and lift. The geometric angle of attack is defined as $\alpha = \alpha_i + \alpha_{eff}$. Secondly the downward deflection of the free jet caused by the wing needs to be taken into account. This effect is dependant on the ratio between the height of the wind tunnel and the chord length of the wing, and described by Glauert [9]. The ultimate downward velocity w_0 is defined as

$$w_0 = v\frac{c}{h}c_l$$

where h is the height of the wind tunnel, v the wind speed, c the chord length and c_l the measured lift coefficient. The adjusted lift coefficient can be calculated as

$$c_l = \pi(a - a_0 - \frac{1}{2}\frac{c}{h}c_l)$$
$$c_l = c_l(f) - \frac{\pi}{2}\frac{c}{h}c_l$$

where a_0 is the angle of zero lift, a is the geometric angle of attack, and $c_l(f)$ is the lift coefficient predicted by xfoil. Therefore the new lift force is calculated to be

$$\frac{L_0}{C_L} = 1 + \frac{\pi}{2}\frac{c}{h}$$

where L_0 is the lift in the unlimited stream, and C_L is the lift in the free stream of the open wind tunnel. The combination of the above equations results in the corrected lift and drag

$$\frac{L_0}{C_L} = 1 + \frac{\pi}{2}\frac{c}{h} + \frac{\pi^2}{12}(\frac{c}{h})^2 = 2.64$$
$$C_D = c_d + \frac{1}{2}\frac{c}{h}C_L^2$$

Therefore the measured lift force needs to be multiplied by 2.64. The drag needs to be adjusted individually depending on the measured lift force and the predicted drag coefficient.

3.3 Test Results and Evaluation

The measured data is adjusted using the correction factors described in Section 3.2. In Figure 9 the corrected lift curves of the finite and infinite end-plates are compared to the predicted xfoil curves. Due to the loss of lift at the wing tips, the finite end-plate setup generates less lift compared to the infinite end-plate setup. The match between the measured curves and the predicted values is better at lower angles up to 12°. At high angles, above 15°, the results spread due to air flow separation. For the NACA9315, the air flow separates earlier at low wind speeds, as shown in Figure 8.

The measured drag curves and the adjusted xfoil predictions for the five tested profiles are shown in Figure 10. The drag of the infinite end-plates is generally higher, as the end-plates are connected to the balance and add to the measured drag force. Furthermore, the airflow changes its angle over the length of the chord and is not parallel to the balance. Therefore some of the measured drag is a result of the generated lift. The xfoil predicted drag and the measured drag have a worse match than for the lift curves, as the measured forces are smaller and less accurate. Furthermore factors, such as the induced drag and the end-plates add to the uncertainty of the measurements.

The achieved shape of the wing slightly differs from the shapes which were used for the xfoil predictions. Figure 11 shows the difference between the NACA9315 predicted outline and the real outline. This is due to the rigid wingbox, and the fact, that the compartment plates expand in a straight line. However, for the lift and drag curves it is shown, that the wing generates approximately as much lift and drag as predicted with xfoil. The generated lift forces change according to the change in airfoil shape. Furthermore the overall range of lift coefficient is much greater than for conventional wings.

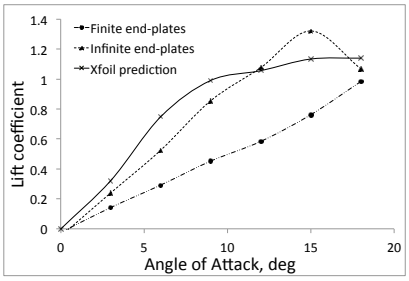

(a) Lift curve of NACA 0015

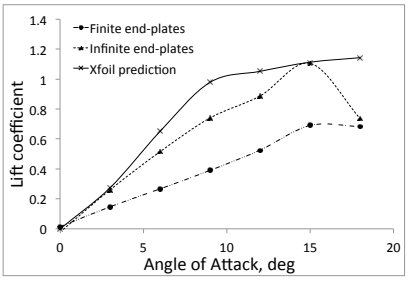

(b) Lift curve of NACA 0018

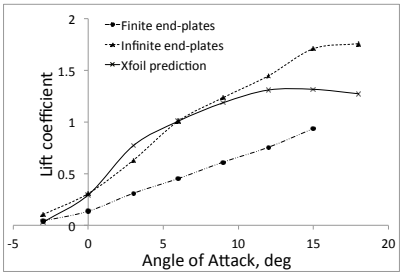

(c) Lift curve of NACA 3315

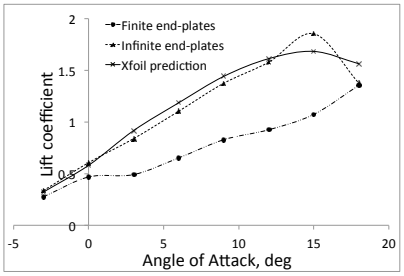

(d) Lift curve of NACA 6315

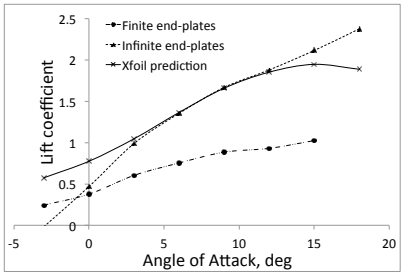

(e) Lift curve of NACA 9315

Figure 9. Lift curve comparison of finite and infinite end-plate setups and the xfoil predictions

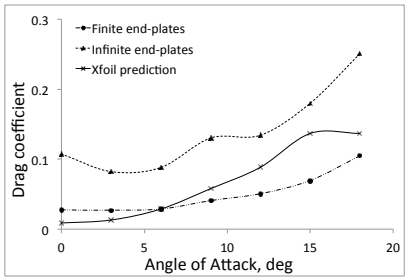

(a) Drag curve of NACA 0015

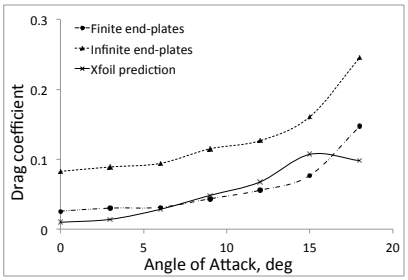

(b) Drag curve of NACA 0018

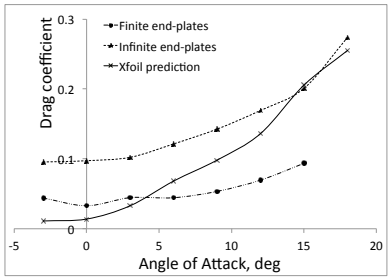

(c) Drag curve of NACA 3315

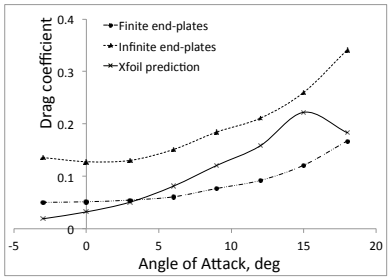

(d) Drag curve of NACA 6315

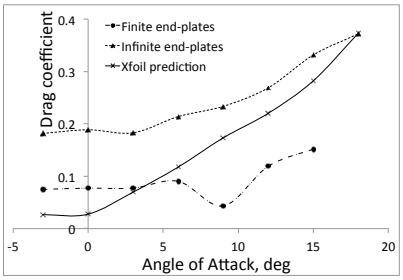

(e) Drag curve of NACA 9315

Figure 10. Drag curve comparison of finite and infinite end-plate setups and the corrected xfoil predictions

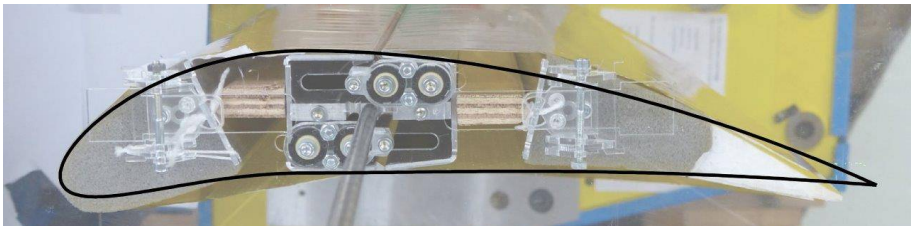

Figure 11. Difference between predicted outline and test wing outline for NACA9315 profile

4. CONCLUSION

During the project, a new concept for morphing wings was developed and tested. The concept allows for controlled changes of the chord length by 25% and camber changes of 9% of the original chord length. The deflection of the foam sections due to aerodynamic loads was minimal, while the measured lift coefficients are close to the predicted values. However, the achieved shapes had certain deviation of the predicted values due to the internal structure. Furthermore the measured drag had certain inaccuracies due to the test setup.

REFERENCES

1. A.Y.N. Sofla and S.A. Meguid and K.T. Tan and W.K. Yeo, "Shape morphing of aircraft wing: Status and challenges", Materials and Design, Vol. 31, No. 3, pp.1284-1292, 2009
2. Silvestro Barbarino and Onur Bilgen and Rafic M. Ajaj and Michael I. Friswell and Daniel J. Inman, "A Review of Morphing Aircraft, Journal of Intelligent Material Systems and Structures, Vol. 22, No.9 823-877, 2011
3. John S. Flanagan and Rolf C. Strutzenberg and Robert B. Myers and Jeffrey E. Rodrian, "Development and Flight Testing of a Morphing Aircraft, the NextGen MFX-1", 48th AIAA/ASME/ASCE/AHS/ASC Structures, Structural Dynamics, and Materials Conference, 2007
4. Edmund W. Pendleton and Denis Bessette and Peter B. Field and Gerald D. Miller and Kenneth E. Griffin, "Active Aeroelastic Wing Flight Research Program: Technical Program and Model Analytical Development", Journal of Aircraft, Vol. 37, No.4 pp. 554-561, 2000
5. R.M. Barrett and R.S. Gross and F.T. Brozoski, "Design and Testing of a Subsonic All-Moving Adaptive Flight Control Surface", AIAA Journal Vol.35, No.7, 1997
6. Matthew G. Good, "Development of a Variable Camber Compliant Aircraft Tail using Structural Optimization", Virginia Polytechnic Institute and State University, July 2003
7. Qunli Liu and Ghatu Subhash, "A Phenomenological Constitutive Model for Foams Under Large Deformations", Polymer Engineering and Science Vol.44, No.3, pp.463-473, 2004
8. C. Thill and J. Etches and I. Bond and K. Potter and P. Weaver, "Morphing skins", The Aeronautical Journal, Vol. 112, No. 1129, 2008
9. H. Glauert, "Wind Tunnel Interference in Wings, Bodies and Airscrews", Aeronautical Research Committee No 1566, 1933